

## Photocatalytic degradation of azo reactive dyes with ultraviolet and sunlight irradiated zinc oxide

Aba Akebi Atta-Eyison<sup>a</sup>, Samuel Tetteh<sup>b</sup>, Ruphino Zugle<sup>b,\*</sup>

<sup>a</sup>Department of Textile Technology, Takoradi Technical University, Ghana.

<sup>b</sup>Department of Chemistry, School of Physical Sciences, College of Agriculture and Natural Sciences, University of Cape Coast, Ghana.

Received: 11 December 2019

Accepted: 24 February 2020

Published online: 20 April 20

**Abstract** Dye effluents are among the most persistent sources of pollution of water bodies and aquatic life. Notable dyes with known carcinogenic effects at low concentrations include azo reactive dyes. The present investigation is focused on the photocatalytic degradation of representative commercial azo dyes using zinc oxide (ZnO). The findings of this research show that ZnO irradiated with ultraviolet (UV) radiation is more effective at degrading C.I. Reactive Yellow 145, C.I. Reactive Blue 194 and C.I. Reactive Red 194 as compared to the sunlight irradiated ZnO. The crystallinity, surface morphology and band gap energy of the ZnO were characterized by X-ray diffraction (XRD), scanning electron microscopy (SEM) image and UV-Visible absorption spectroscopy respectively. The ZnO has a hexagonal wurzite structure with a band gap of 3.17 eV. The degradation profile was found to decrease with increasing initial dye concentration. The degradation efficiency of the respective dyes under UV and sunlight irradiation was found to be 90% and 85% for CIRY145; 88% and 82% for CIRB194; 96% and 90% for CIRR194. Optimum degradation pH values of 6.9, 7.2 and 6.2 were also recorded for CIRY145, CIRB and CIRR194, respectively, and the general degradation profile was found to follow first order kinetics. Gas chromatographic studies of the degradation reaction intermediates also showed that the degradation profile is time-dependent and all potentially carcinogenic intermediates were degraded into smaller environmentally friendly products such as oxalic acid and acetic acid.

**Keywords:** Azo reactive dye; photocatalytic degradation; UV-Visible light irradiation; sunlight; Zinc oxide photocatalyst.

### 1. Introduction

The release of textile effluents into water bodies has been of great environmental concern [1]. Azo dyes, in particular, account for approximately 60-70% of all dyes used in textile manufacture and represent about 60% of all reactive dyes used by the textile industry [2, 3]. The existence of azo dyes and their intermediates in water bodies lead to intolerable coloration as well as the reduction of sunlight penetration, photosynthetic activity, dissolved oxygen levels and associated death of aquatic animals [4, 5]. Partially degraded azo dyes have also been reported to be toxic, carcinogenic, neurotoxic and genotoxic [6-8].

Under typical reactive dyeing conditions, up to 50% of the initial dye remains in the dye bath which results in a coloured effluent [9-11]. These dyes are known to be nondegradable under the typical aerobic conditions found in conventional-biological treatment systems and are adsorbed very poorly on biological solids, resulting in residual colour in the discharged effluents [12, 13]. Recently, heterogeneous photocatalysis, an advance oxidation process (AOP), has shown promising results of complete degradation of dye compounds into harmless substances using insoluble semiconductors [8]. These methods involve the in situ generation of powerful oxidizing agents such as hydroxyl radicals of sufficient concentrations in order to effectively degrade harmful water pollutants [14].

Daneshvar et al recently reported that ZnO semiconductor has comparable potential as an alternative for TiO<sub>2</sub> to efficiently

degrade azo dyes and aromatic compounds in aqueous solutions [15]. According to their work, the UV irradiated ZnO catalytic process is very efficient in degrading acid red 4, although ZnO and UV light have negligible effects when used separately. This is because the ultraviolet light has the required amount of energy to photoexcite electrons in the ZnO structure. Afterwards, these photoexcited electron-hole pairs initiate redox processes with water and oxygen to degrade organic pollutants. Several ZnO-based catalytic modifications have also been successfully utilized for the photocatalytic degradation of a wide range of organic dyes with high efficiency and activity using solar irradiation [11]. With good photocatalytic activity, versatile morphologies, and an open and modifiable crystalline structure, ZnO has therefore become an excellent photocatalyst for the degradation of organic pollutants [16, 17].

In this study, the feasibility of using ZnO catalyst for the degradation of CIRY145, CIRB194 and CIRR194 in an aqueous medium has been investigated. Factors such as the effect of pH and initial dye concentration were also studied. The degradation efficiency under both ultraviolet and sunlight irradiation were also assessed. The degradation products of the dyes were also studied using the gas chromatography coupled with a mass spectrometer detector. Finally, the kinetics of the degradation process were also investigated.

### 2. Experimental

#### 2.1. Dyes

Commercially available water soluble azo reactive dyes (CIRY145, CIRR194 and CIRB194) were obtained from a local supplier. The necessary information related to these dyes were obtained from Shaoming Bing Textile Technology Co., Ltd. and Sigma-Aldrich, Inc. The dyes were used without further purification. The chemical structures are presented as supplementary materials.

#### 2.2. Reagents and chemicals

All chemicals were of analytical grade with the exception of acetonitrile, which was HPLC grade, and were used without further purification. Zinc oxide powder, hydrochloric acid and sodium hydroxide were purchased from Central Drug House (P) Ltd. Acetonitrile was purchased from Daejung Chemicals & Metals Co. Ltd. Dimethyl sulfoxide, ethanol and hexane were also purchased from VWR Chemicals, Spain.

#### 2.3. Photocatalytic activity of ZnO/UV

Photocatalytic activity of ZnO catalyst was studied on CIRY45, CIRB194 and CIRR194 as model pollutants. The experiment was carried out by adding 5 mg of ZnO to 100 mL of dye solution in a 150 mL beaker. This set up was placed on a magnetic stirrer in a Chromato-Vue cabinet C-70G and irradiation at 365 nm. The suspension was continuously stirred at 300 rpm using a magnetic stirrer. Exactly 5 mL of the suspension was withdrawn every 20 minutes for 140 minutes and filtered. The absorption spectra of the filtered samples were subsequently analyzed using a JENWAY

7315 Spectrophotometer. The whole experiment was repeated under direct sunlight at 20000 lux intensity. The dye degradation efficiency was calculated using Eq. (1).

$$\text{Dye degradation efficiency (\%)} = \frac{C_0 - C_t}{C_0} \times 100 \% \quad (1)$$

Where  $C_0$  is the initial concentration (mg/L) of the dye,  $C_t$  is the concentration at a given time.

The effect of initial dye concentration on the degradation efficiency was studied by varying the initial concentration of the dyes as follows; CIRY145 (100 mg/L, 200 mg/L, 300 mg/L), CIRB194 (50 mg/L, 100 mg/L, 150 mg/L) and CIRR194 (100 mg/L, 200 mg/L, 300 mg/L). The effect of pH on the various dye degradation efficiency was also studied between pH 3-10. The pH of the solution was adjusted using 1.0 M HCl and 1.0 M NaOH solution.

### 3. Results and discussion

#### 3.1. Absorption analysis of dyes

Figure 1 shows the UV-Vis spectra of the respective dyes in distilled water. The absorption spectra were measured between 300-800 nm. CIRY145 had a maximum absorbance wavelength at 420 nm, CIRB194, 620 nm with CIRR194 recording  $\lambda_{\text{max}}$  of 520 nm. These values are consistent with their complementary colours [18]

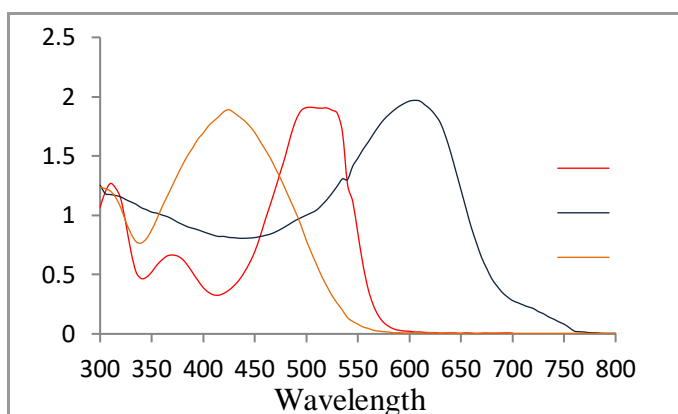


**Figure 1.** UV-Vis Absorption Spectra of (a) CIRY145, (b) CIRR194 and (c) CIRB194.

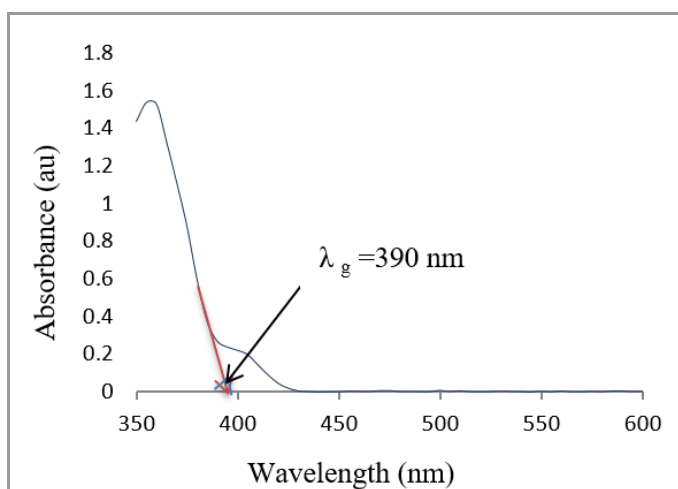


**Figure 2.** UV-Visible Absorption Spectrum of ZnO determined in ethanol.

#### 3.2. Physical characterization of ZnO

The wide band gap energy ( $E_g$ ) of ZnO is the basis for its photocatalytic activity [15]. As shown in Figure 2, the wavelength

of the cut-off edge ( $\lambda_g$ ) was found to be 390 nm which was used to calculate the  $E_g$  in equation 2 [19].

$$E_g = \frac{1240}{\lambda_g} \quad (2)$$

Where,  $E_g$  = band gap energy in electron volt (eV) and  $\lambda_g$  = absorption edge of ZnO in nanometers (nm). The calculated  $E_g$  of 3.17 eV agreed strongly with the value of  $E_g$  = 3.2 eV reported in the literature [19, 20].

The XRD pattern of ZnO recorded on an Empyrean X-ray Diffractometer using the standard Empyrean platform with the high resolution theta-theta goniometer diffractometer is shown in Figure 3. The main diffraction peaks were observed at  $2\theta$  angles of 31.82°, 34.47°, 36.29°, 47.59°, 56.65°, 62.88°, 66.38°, 67.99° and 69.14°. These peaks matched sturdily with the diffraction planes of (100), (002), (101), (102), (110), (103), (200), (112) and (201), respectively. All the diffraction peaks can be indexed as the typical hexagonal wurtzite with lattice constants reported elsewhere [21]. The sharp diffraction peaks can be regarded as an indication of the high crystallinity of the ZnO [22, 23]. This characteristic feature can improve its catalytic performance by impeding electron/hole ( $e^-/h^+$ ) pair recombination and producing more reactive species for effective reaction with target pollutant [8, 24].

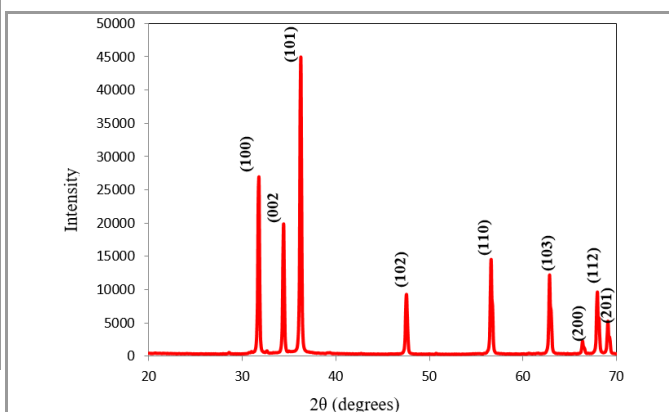


**Figure 3.** XRD pattern of ZnO showing characteristic diffraction peaks indexed to the hexagonal wurtzite structure.

The surface morphology (shown in figure 4) was observed at X850 and X3500 magnifications using a JOEL JSM-6390 LV scanning electron microscope. The particles look aggregated at high magnifications with most of them assembling into branched and urchin-like structures [25]. This provides a high surface area suitable for catalysis.

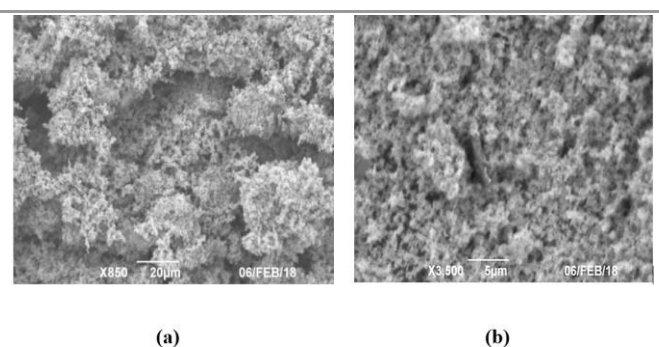


**Figure 4.** SEM Image of Zinc Oxide at Magnification of (a) X 850 and (b) X 3,500.

Figure 5 shows the degradation profile of the respective dyes when irradiated under UV light at 365 nm in the presence of the ZnO. The main peaks observed in the visible region include 420 nm for CIRY145, 610 nm for CIRB194 and 520 nm for CIRR194. Generally, these bands decreased gradually as the exposure time increased and disappeared after 140 minutes of irradiation. The decrease in absorbance indicated the reduction of dye concentration in various solutions as a result of the breakdown of the dye molecules into colourless species.

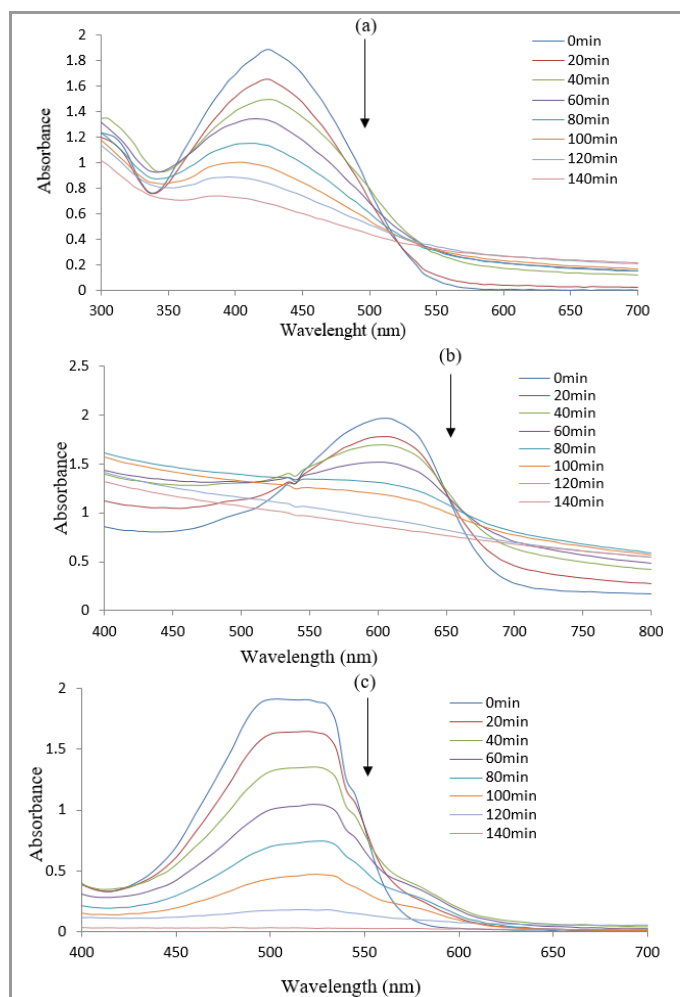


**Figure 5.** UV-Vis degradation profile of 3 mg/L concentration of the respective dye solutions with 5 mg ZnO (a) CIRY145 (b) CIRB194 (c) CIRR194.

### 3.3. Comparative degradation studies

The degradation efficiency was also assessed in sunlight relative to that observed in figure 6 under UV-light irradiation. This was done because of the relative abundance of sunlight energy and the ability of ZnO to convert solar energy into chemical energy [26]. As shown in figure 6, the degradation efficiency increased steadily in the course of the experiment. Generally, the UV light which activated the catalytic process gave higher efficiencies than the sunlight activated catalysis. Degradations of 90% and 85% were recorded for CIRY145 under UV light and sunlight respectively, 88% and 82% for CIRB194 with CIRR194 giving the highest of 96% and 90%. These competitive catalytic activity of ZnO in sunlight can however be enhanced by modifications such as the addition of co-catalysts [27].

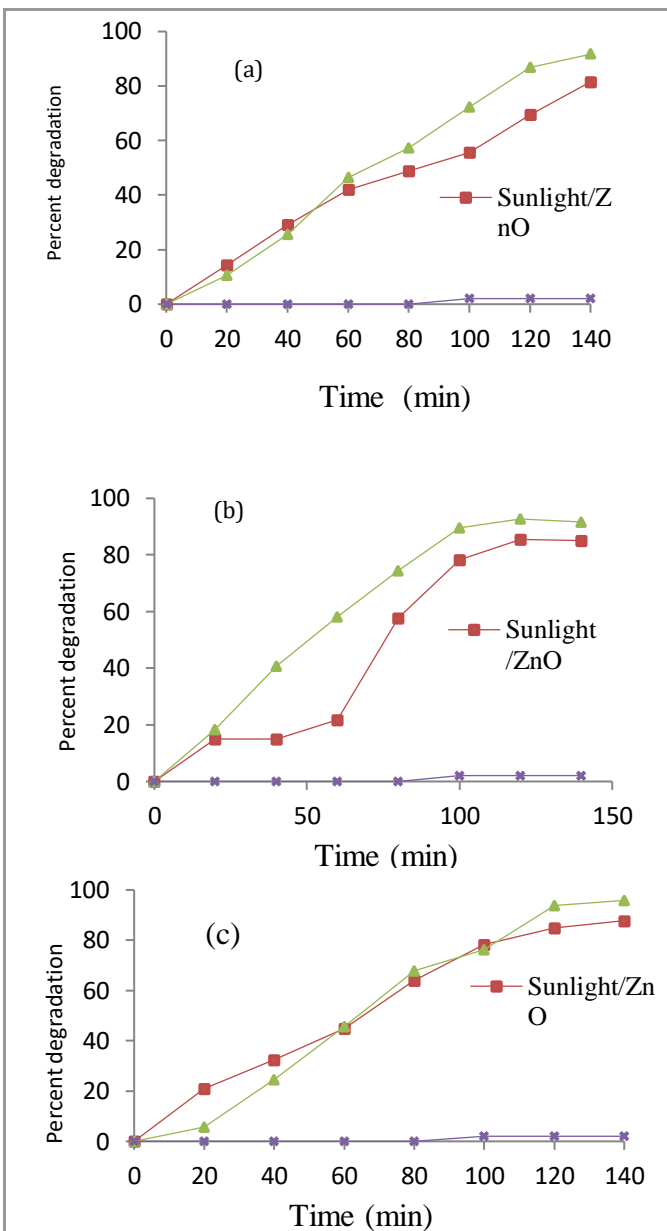


**Figure 6.** Time-dependent degradation of the dye samples under various conditions (Photocatalyst loading = 5 mg) (a) CIRY145 (b) CIRB194 (c) CIRR194.

Generally, there was insignificant degradation of the dyes in darkness. The low percentages recorded after 140 minutes could be attributed to the adsorptive properties of ZnO which contributed to the removal of some of the dyes from the solution [28].

### 3.4. Effect of Initial Dye Concentration

Based on the account that the industrial waste water usually contains different dye concentrations, it is crucial to investigate the effect of the initial dye concentration on the degradation process. The influence of initial dye concentration was determined by preparing different dye concentrations. Figure 7 shows the effect of initial dye concentration of the various dyes under UV irradiation.

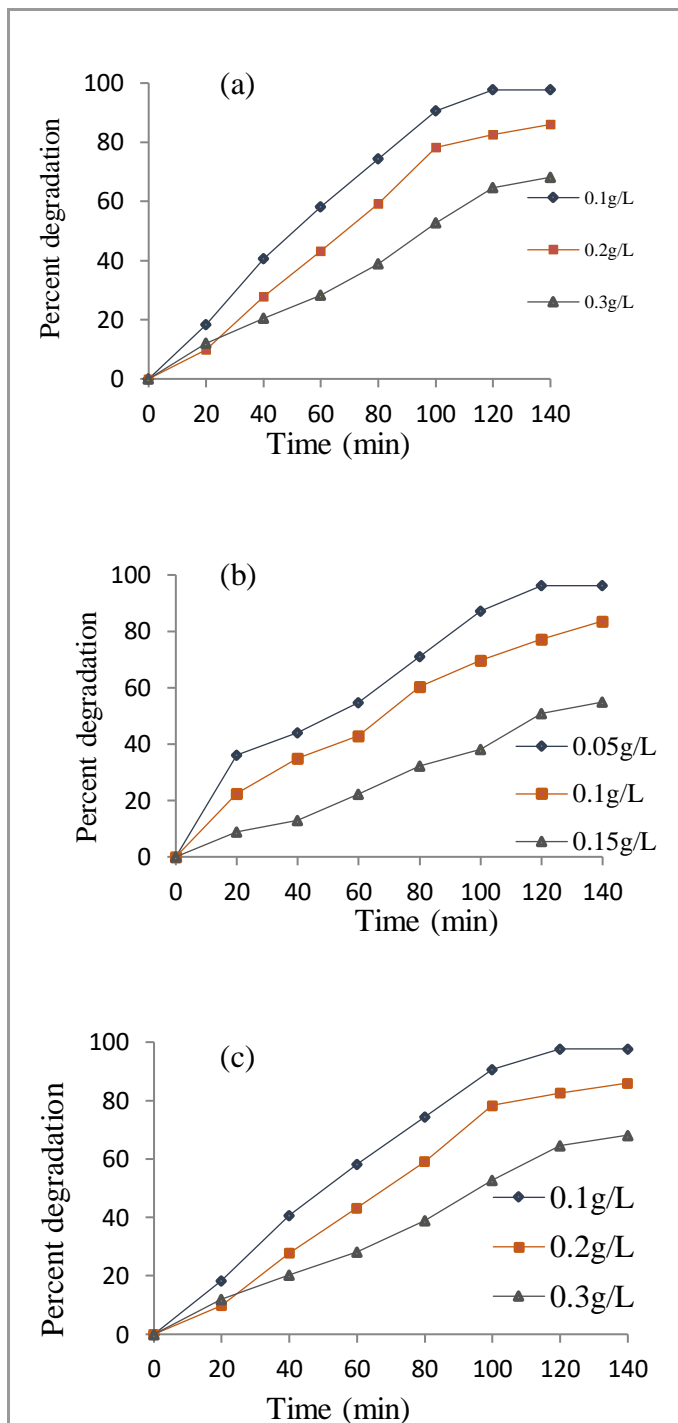


**Figure 7.** Degradation profile of the samples at different initial dye concentrations (ZnO Loading = 5 mg) (a) CIRY145 (b) CIRB194 (c) CIRR194.

It can be observed from figures 7 (a), (b) and (c) that the degradation percentage decreased with increasing the initial dye concentrations. Increasing the dye concentration increases the colour intensity of the solution which leads to interception of photons before reaching the surface of the catalyst [20]. The lower light penetration causes ineffective irradiation of ZnO which resulted in lower degradation efficiencies. The concentration of dye is also proportional to the number of dye molecules that get adsorbed onto the surface of the photocatalyst [29]. When the concentration of dye is high, the amount of available active sites for the reaction between active radicals and dye molecules decrease because of the competitive adsorption of dye molecules on the ZnO surface.

### 3.4. Effect of Solution pH

The initial pH is very important in the photocatalytic process. Under optimum condition of 0.3 g/L CIRY145, 0.1 mg/L CIRB194 and 0.15 g/L CIRR194 with 0.005 g/L ZnO loading, the effect of the pH on the degradation of the dyes was studied by varying the solution pH from 3.2 to 10.4. The values of solution pH were chosen based on the different conditions such as acidic, natural, neutral and alkaline media. Figure 8 represents the effect of solution pH on the photocatalytic degradation of dyes.

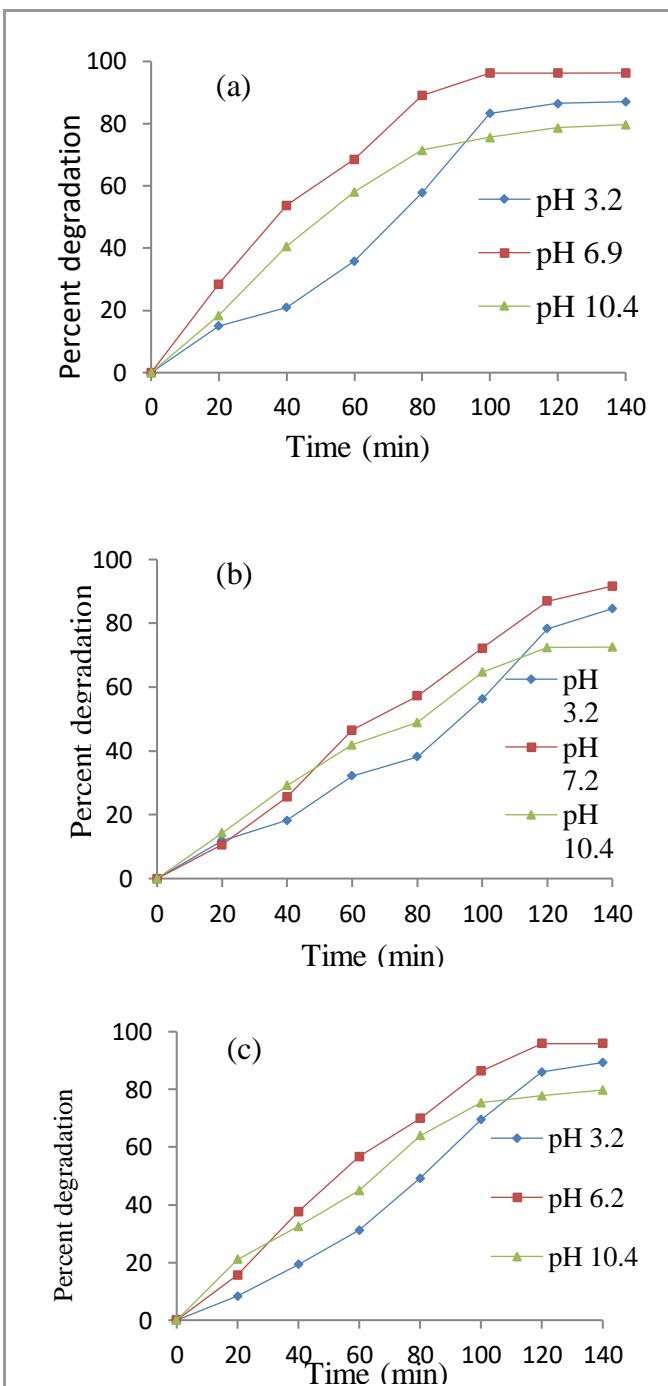


**Figure 8.** Effect of pH on the degradation profile of the respective dyes (ZnO loading = 0.005 g/L) (a) CIRY145 concentration of 0.3g/L (b) CIRB194 concentration of 0.15g/L (c) CIRR194 concentration of 0.1g/L.

The results clearly show that the degradation of the dyes was mostly effective at pH values of 6.9 (a), 7.2 (b) 6.2 (c), respectively. At pH

below pH 7, foraging of  $\bullet\text{OH}$  by  $\text{H}^+$  was dominant due to the presence of high amounts of  $\text{H}^+$  in acidic condition. This enhanced the adsorption of anionic dye molecules onto the surface of the ZnO where degradation took place. Foraging of  $\bullet\text{OH}$  by  $\text{H}^+$  was therefore likely to be dominant at pH 3.2 which caused a drop in photocatalytic degradation percentages of the dyes. At the natural pH, the foraging of  $\bullet\text{OH}$  is less prevailing as no pH adjustment was performed which indicated that there was no addition of  $\text{H}^+$  into the dye solution. This evidently explained the higher degradation percentage at the natural pH of the dyes as compared to that at pH 3.2. At pH 10.4. The surface of the ZnO was negatively-charged which created electrostatic repulsion between dye molecules, other anions such as  $\text{OH}^-$  and the negatively-charged surface of ZnO. This possibly reduced the degradation of the dye molecules on the surface of the photocatalyst and production of  $\bullet\text{OH}$  through the reaction of  $\text{OH}^-$  and  $\text{h}^+$  [15].

### 3.4. Effect of initial dye concentration on rate of degradation

Figure 9 shows a plot of  $\ln \text{Co/C}$  vs.  $t$  of the dyes at different initial dye concentrations which give a straight line indicating a first order kinetic reaction.

The observed rate constants ( $K_{\text{obs}}$ ) and correlation coefficient ( $R^2$ ) at different initial concentrations are summarized in Table 1. From these results,  $K_{\text{obs}}$  is inversely proportional to the initial concentration for all dyes which agree to what has been previously reported in the literature [8, 17]. This decrease was due to the increase in initial dye concentrations which led to higher interaction between dye molecules in adsorbing onto the surface of the photocatalyst.

### 3.4. GC-MS analysis

Following the time dependent changes in concentration of the respective dyes observed in figures 5-7, six degradation intermediates of CIRY145 were monitored to understand the degradation profile of the process. These intermediates include 1,2,6-Naphthalenetriol (a), phthalic acid (b), 1,4-benzoquinone (c), nitrobenzene (d), oxalic acid (e) and acetic acid (f). As shown in table 2, all these intermediates were observed in the filtrate up to the first 60 minutes of the experiment. Subsequently, only c, d, e and f were observed for the next 80 minutes of reaction.

This shows that 1,2,6-naphthalenetriol and phthalic acid were degraded into simpler products as the reaction proceeded. After 140 minutes, all the potentially carcinogenic (benzenoid) intermediates had been degraded into oxalic acid and acetic acid. Comparison of the intermediates recorded in table 2 suggests that an increase in the reaction time leads to an increase in the degradation of CIRY145 into smaller environmentally friendly products.

## Conclusion

ZnO photocatalyst was effective in the degradation of the C.I Reactive Yellow 145, C.I Reactive Blue 194 and C.I Reactive Red 194 both under UV light irradiation and in sunlight. There was relatively insignificant degradation of the dye samples in the dark even in the presence of ZnO. Under the experimental conditions, the efficiency of degradation of the dyes increased with decreasing the initial concentrations of the dyes. Optimum degradation efficiency was achieved at the natural pH of the dyes. Analysis of the degradation intermediates showed that the degradation of CIRY145 was time-dependent and all potentially carcinogenic intermediates were degraded into smaller environmentally friendly products such as oxalic acid and acetic acid.

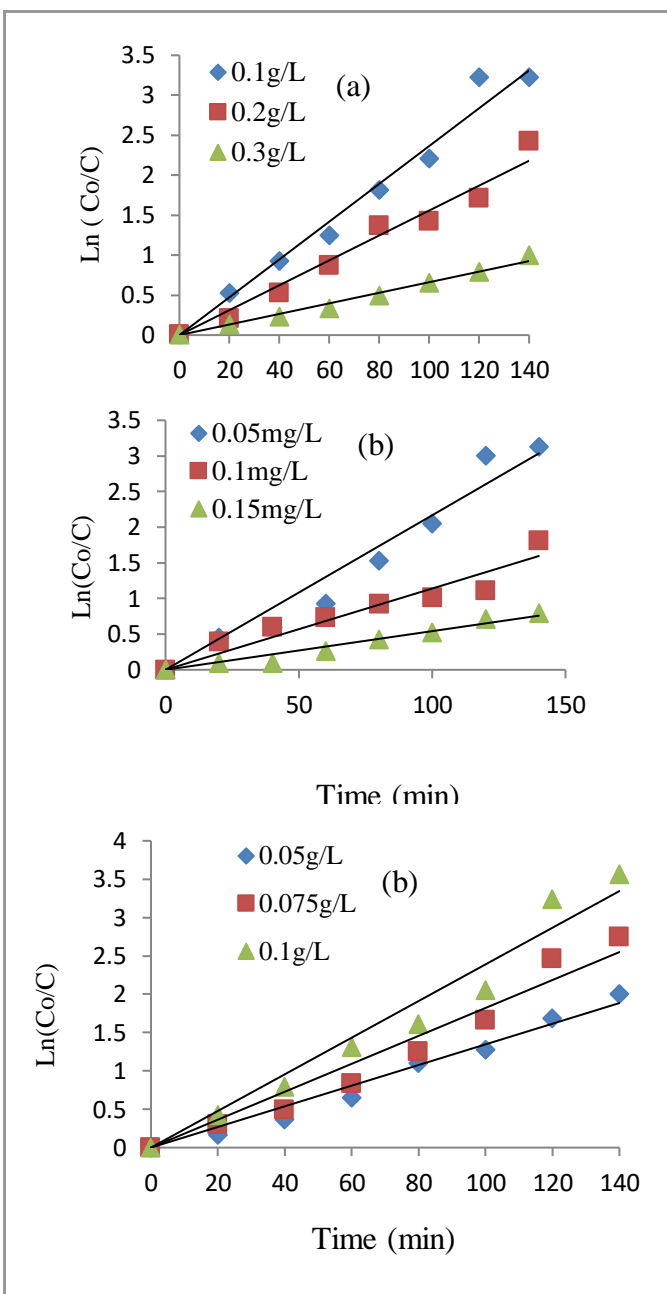


**Figure 9.** Kinetics of Photocatalytic Degradation of the respective dyes. (ZnO loading = 5 mg/L). (a) CIRY145 at solution pH of 6.9 (b) CIRB194 at solution pH of 7.2 (c) CIRR194 at solution pH of 6.2.

**Table 1.** The  $K_{\text{obs}}$  and  $R^2$  values at different initial dye concentrations.

Dye	Initial concentration(mg/L)	$K_{\text{obs}}$	$R^2$
		( $\text{min}^{-1}$ )	
CIRY145	0.1	0.0237	0.9779
	0.2	0.0156	0.9696
	0.3	0.066	0.9849

CIRB194	0.05	0.0217	0.9543
	0.1	0.0114	0.9134
	0.15	0.0054	0.9604
CIRR194	0.05	0.0239	0.9620
	0.075	0.0182	0.9563
	0.1	0.0133	0.9751

### Conflicts of interest

The authors declare that there is no conflict of interest regarding the preparation and publication of this manuscript.

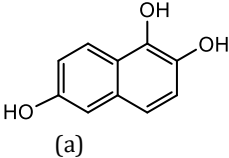
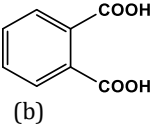
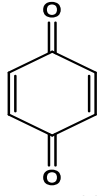
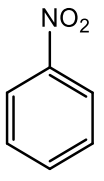
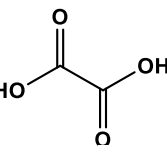
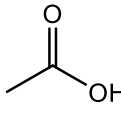
### Data availability statement

All data used for this work are available from the corresponding author upon request.

### Funding statement

No external source of funding was assessed for this work. The work was conducted as a requirement of the authors' employment and academic research.

**Table 2.** Identified degradation intermediates of CIRY145 by GC-MS.

Irradiation time (min)	Identified reaction intermediates					
20						
40	(a)	(b)	(c)	(d)	(e)	(f)
60	(a)	(b)	(c)	(d)	(e)	(f)
80			(c)	(d)	(e)	(f)
100			(c)	(d)	(e)	(f)
120				(d)	(e)	(f)
140					(e)	(f)

### References

- De Moraes, S.G., R.S. Freire, and N. Duran, Degradation and toxicity reduction of textile effluent by combined photocatalytic and ozonation processes. *Chemosphere*, 2000. 40(4): p. 369-373.
- Gözmen, B., et al., Oxidative degradations of reactive blue 4 dye by different advanced oxidation methods. *Journal of Hazardous materials*, 2009. 168(1): p. 129-136.
- Dalvand, A., et al., Modeling of Reactive Blue 19 azo dye removal from colored textile wastewater using L-arginine-functionalized Fe<sub>3</sub>O<sub>4</sub> nanoparticles: Optimization, reusability, kinetic and equilibrium studies. *Journal of Magnetism and Magnetic Materials*, 2016. 404: p. 179-189.
- Agarwal, R., D.W. Denning, and A. Chakrabarti, Estimation of the burden of chronic and allergic pulmonary aspergillosis in India. *PLoS One*, 2014. 9(12): p. e114745.
- Khehra, M.S., et al., Biodegradation of azo dye CI Acid Red 88 by an anoxic-aerobic sequential bioreactor. *Dyes and Pigments*, 2006. 70(1): p. 1-7.
- Carmen, Z. and S. Daniela, Textile organic dyes—characteristics, polluting effects and separation/elimination procedures from industrial effluents—a critical overview. in *Organic pollutants ten years after the Stockholm convention-environmental and analytical update*. 2012. InTech.
- de Lima, R.O.A., et al., Mutagenic and carcinogenic potential of a textile azo dye processing plant effluent that impacts a drinking water source. *Mutation Research/Genetic Toxicology and Environmental Mutagenesis*, 2007. 626(1): p. 53-60.
- Luk, M.K., Photocatalytic Degradation and Chlorination of Azo Dye in Saline Wastewater, 2016. UTAR.
- uO, D.O., A. Osuntoki, and G. Gbenle, Decolourization of azo dyes by a strain of *Micrococcus* isolated from a refuse dump soil. *Biotechnology*, 2009. 8(4): p. 442-448.
- Kannan, S., K. Dhandayuthapani, and M. Sultana, Original Research Article Decolorization and degradation of Azo dye-Remazol Black B by newly isolated *Pseudomonas putida*. *Int. J. Curr. Microbiol. App. Sci*, 2013. 2(4): p. 108-116.
- Lam, S.-M., et al., Degradation of wastewaters containing organic dyes photocatalysed by zinc oxide: a review. *Desalination and Water Treatment*, 2012. 41(1-3): p. 131-169.
- Jo, W.-K. and R.J. Tayade, Recent developments in photocatalytic dye degradation upon irradiation with energy-efficient light emitting diodes. *Chinese Journal of Catalysis*, 2014. 35(11): p. 1781-1792.
- Zangeneh, H., et al., Photocatalytic oxidation of organic dyes and pollutants in wastewater using different modified titanium dioxides: a comparative review. *Journal of Industrial and Engineering Chemistry*, 2015. 26: p. 1-36.
- Oturan, M.A. and J.-J. Aaron, Advanced oxidation processes in water/wastewater treatment: principles and applications. A review. *Critical Reviews in Environmental Science and Technology*, 2014. 44(23): p. 2577-2641.
- Daneshvar, N., D. Salari, and A. Khataee, Photocatalytic degradation of azo dye acid red 14 in water on ZnO as an alternative catalyst to TiO<sub>2</sub>. *Journal of photochemistry and photobiology A: chemistry*, 2004. 162(2-3): p. 317-322.
- Hernández-Alonso, M.D., et al., Development of alternative photocatalysts to TiO<sub>2</sub>: challenges and opportunities. *Energy & Environmental Science*, 2009. 2(12): p. 1231-1257.

- [17] Subash, B., et al., An efficient nanostructured Ag<sub>2</sub>S–ZnO for degradation of Acid Black 1 dye under day light illumination. *Separation and Purification Technology*, 2012. 96: p. 204-213.
- [18] Park, H.J., et al., Photonic color filters integrated with organic solar cells for energy harvesting. *ACS Nano*, 2011. 5(9): p. 7055-7060.
- [19] Jia, Z., et al., Photocatalytic degradation and absorption kinetics of cibacron brilliant yellow 3G-P by nanosized ZnO catalyst under simulated solar light. *Journal of the Taiwan Institute of Chemical Engineers*, 2016. 60: p. 267-274.
- [20] Mirzaei, A., et al., Removal of pharmaceuticals and endocrine disrupting compounds from water by zinc oxide-based photocatalytic degradation: a review. *Sustainable Cities and Society*, 2016. 27: p. 407-418.
- [21] Chenari, H.M., H.F. Moafi, and O. Rezaee, A study on the microstructural parameters of Zn (1-x) La<sub>x</sub>Zr<sub>x</sub>O nanopowders by X-ray line broadening analysis. *Materials Research*, 2016. 19(3): p. 548-554.
- [22] Bindu, P. and S. Thomas, Estimation of lattice strain in ZnO nanoparticles: X-ray peak profile analysis. *Journal of Theoretical and Applied Physics*, 2014. 8(4): p. 123-134.
- [23] Yu, L., et al., Decolorization characteristics of a newly isolated salt-tolerant *Bacillus* sp. strain and its application for azo dye-containing wastewater in immobilized form. *Applied microbiology and biotechnology*, 2015. 99(21): p. 9277-9287.
- [24] Kee, M.W., Enhanced Photodegradation of Dye Mixtures (Methyl Orange and Methyl Green) and Real Textile Wastewater by ZnO Micro/Nanoflowers, 2017, UTAR.
- [25] Polsongkram, D., et al., Effect of synthesis conditions on the growth of ZnO nanorods via hydrothermal method. *Physica B: Condensed Matter*, 2008. 403(19-20): p. 3713-3717.
- [26] Roselin, L.S., et al., Sunlight/ZnO-mediated photocatalytic degradation of reactive red 22 using thin film flat bed flow photoreactor. *Solar Energy*, 2002. 73(4): p. 281-285.
- [27] Wang, D., et al., Enhanced photocatalytic activity of TiO<sub>2</sub> under sunlight by MoS<sub>2</sub> nanodots modification. *Applied Surface Science*, 2016. 377: p. 221-227.
- [28] Wu, J.-J., et al., Effects of dye adsorption on the electron transport properties in ZnO-nanowire dye-sensitized solar cells. *Applied Physics Letters*, 2007. 90(21): p. 213109.
- [29] Ahmed, S., et al., Heterogeneous photocatalytic degradation of phenols in wastewater: a review on current status and developments. *Desalination*, 2010. 261(1-2): p. 3-18.

**How to cite this manuscript:** Aba Akebi Atta-Eyison, Samuel Tetteh, Ruphino Zugle\*, Photocatalytic degradation of azo reactive dyes with ultraviolet and sunlight irradiated zinc oxide. *Frontiers in Chemical Research*, 2020, 2, 26-32. doi: 10.22034/FCR.2020.118439.1015